Journal of KONBiN 2022
Volume 52, Issue 2
DOI 10.2478/jok-2022-0014

Arun Kumar YADAV, Janusz SZPYTKO
AGH University of Science and Technology (Akademia Górniczo-Hutnicza)

METHOD OF INCREASING RELIABILITY OF LARGE DIMENSIONAL BRIDGE-TYPE STRUCTURES

Metoda zwiększenia niezawodności wielkogabarytowych konstrukcji typu mostowego

Abstract: *The paper presents a method of testing the girder of a bridge crane using a specialized measuring type robot. The girder of the bridge crane is an example of a large-size structure. The bridge structure of the crane is a critical subsystem of the transport device due to its operational safety. The purpose of the overhead crane girder tests is to increase the reliability of the structure and operational safety. The proposed solutions indeed comply with the standards in force. Also, they increase their frequency and effectiveness of concluding in terms of predicting possible causes of threats to the safety and reliability of the structure.*
Keywords: overhead crane girder, inspection robot, NDT technology, GMR sensor

Streszczenie: *W artykule przedstawiono metodę badania dźwigara mostu suwnicy pomostowej z użyciem specjalistycznego robota pomiarowego. Dźwigar mostu suwnicy pomostowej jest przykładem konstrukcji typu wielkogabarytowego. Konstrukcja nośna suwnicy jest krytycznym podsystemem środka transportu z uwagi na jego bezpieczeństwo eksploatacyjne. Celem badań dźwigara suwnicy pomostowej jest zwiększenie niezawodności konstrukcji i bezpieczeństwa eksploatacyjnego. Proponowane rozwiązania istotnie wpisują się w obowiązujące przepisami standardy, natomiast umożliwiają zwiększenie ich częstości i skuteczności wnioskowania w zakresie przewidywania możliwych przyczyn zagrożenia bezpieczeństwa i niezawodności konstrukcji.*
Słowa kluczowe: Dźwigar suwnicy, robot inspekcyjny, technologia NDT, czujnik GMR

1. Introduction

Almost all transportation structures necessitate a timely understanding of their structural health to prevent some functional breakdown and, ultimately, catastrophic accidents. Overhead cranes can be found in a variety of locations, including sites outside of civil infrastructure, mechanical infrastructure, and other infrastructure. Some of these overhead crane structures are quite heavy and large, making it impossible to conduct routine health monitoring of them. There are devastating implications when there is a lack of monitoring and inspection. Most of the overhead cranes in seaports operate in an open environment, exposing their surfaces to the elements, direct loading, unloading, and chemical reactions. As a result, regular maintenance is essential to ensure that the cranes continue to operate safely. Currently, the inspector conducts a visual check of the majority of the overhead cranes in the facility. In the visual examination of overhead cranes, they check several main components, such as ropes, hooks, pendent control, and visual cracks. They inspect these parts regularly because they are critical in the operation of cranes. Because of their massive size, it is not practicable to conduct frequent visual inspections of the crane and bridge. Because some crane parts are narrow and out of reach of the inspector, visual examination is not possible on some crane parts due to their design. Overhead cranes mostly run on a special rail mounted under the roof of a production hall, as shown below in fig. 1.

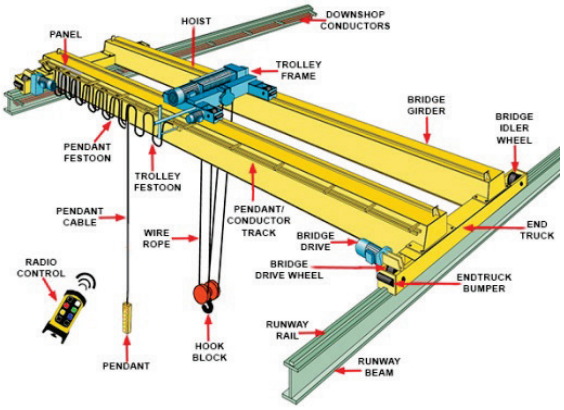

Fig. 1. Overhead crane with double-girder [4]

Despite many technologies and measuring devices, it is tedious to completely identify the root cause of damage to the structure by a particular test method [1, 6, 8, 10]. The majority of non-destructive testing (NDT) procedures are prohibitively expensive when it comes to inspecting huge structures. The overhead cranes in seaports are subjected to

various environmental issues such as humidity and dust, which result in corrosion [5, 11]. Previously, there have been many research methods and testing methodologies that explain single phenomena affecting heavy structures [7, 9, 14]. Many autonomous robots have been designed to perform the inspection task to make the inspection process reliable and safe. In the past years, for wall-climbing robots, some permanent magnetic track components were designed for oil tanks and weld line inspection. Those permanent magnets were used for locomotion of robots [4].

Tache et al. presented a magnetic motorbike robot with two magnetic wheels in a motorbike to climb and inspect the inner casing of ferromagnetic pipes with complex-shaped geometry. The locomotion was based on an adapted magnetic wheel unit integrating two lateral lever arms [15].

Fischer et al. [3] designed a robot to inspect very thin and fragile surfaces based on a pair of the wall-climb robot with magnetic wheels. The robot uses magnetic wheels for adhesion. Some of the robots are equipped with special mechanisms to pass most of the obstacles within their structures. It consists of 10 magnetic wheels in parallel through which they achieved a force of 580 N. Below fig. 2 shows the designed magnetic wheel.

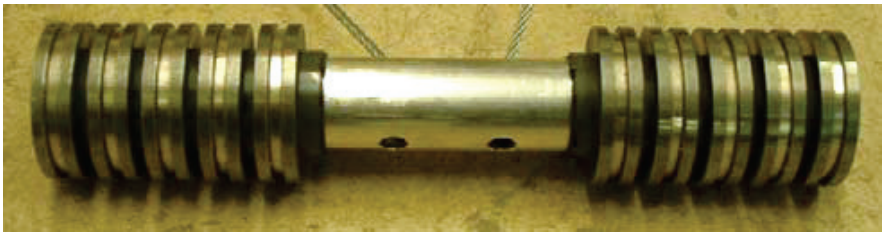

Fig. 2. Magnetic wheel unit [3]

Raul Fernandez et al. [2] presented a wall-climbing robot for tank inspection consisting of magnetic wheels. The magnetic wheel consists of a cylindrical nylon structure in the centre holes that surround the Neodymium (NeFBe) magnet all of which are enclosed in steel plates to pass the magnetic flux on the inspection area.

Mahmoud Tavakoli designed an omnidirectional magnetic wheeled climbing robot to inspect ferromagnetic structures. This robot can be used for flat and convex steel structures. The wheel consists of 14 cylindrical magnets with 12 mm diameter and an adjustable distance [16].

Patrick Schoeneich et al. designed Tubulo - a train-like miniature inspection climbing robot for the inspection of ferromagnetic tubes. Using magnetic wheels, it can climb on tubes of 25 mm diameter and can easily pass through bends with a curvature of 150 mm. The whole robot is segmented into four sections: locomotion section, energy section, communication section, and visual inspection section.

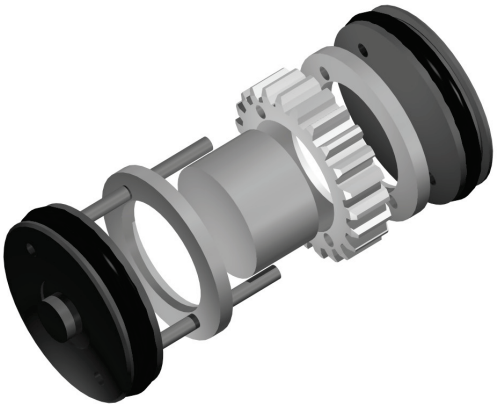

Fig. 3. Design of magnetic wheel centre axis [12]

In the locomotion section as shown above in Fig. 3, the use of a magnetic wheel was chosen instead of any other mechanical adhesion. The designed magnetic wheel consists of a central magnet and two iron flux guides on the sides. The main advantage of the magnetic wheel with a centre axis is that it enhances the holding force. The designed wheel has a diameter of 12 mm and a width of 10 mm. It can hold 2.5 N with rubber seals [12].

The primary goal of this research is to develop an inspection robot that will improve the quality of inspections, speed, and level of safety. This automated robot can inspect the restricted passageways and vertical surfaces of overhead crane bridges. The robot will be equipped with a variety of sensors and cameras that will allow it to capture close-up images of cracks and faults and transmit them to remote places for additional study.

2. Design and Analysis of Robotic System

This section expresses a novel design approach for a climbing inspection robot to detect the defects and flaws in the steel bridges for overhead cranes. The primary research focuses on designing and implementing a cost-economic crack detection robot for the industry to inspect heavy ferromagnetic structures, mainly concentrating on overhead crane bridges. A novel approach is presented to mitigate structural failure and minimize inspection costs by designing an inspection robot with magnetic wheel locomotion. The novelty of the designed robot is the high accuracy rate in detecting the surface and subsurface defects. The lightweight and compact size make this robot design robust and easy to operate. Here, in Fig. 4 below, proposed design of a compact and lightweight robot has been presented.

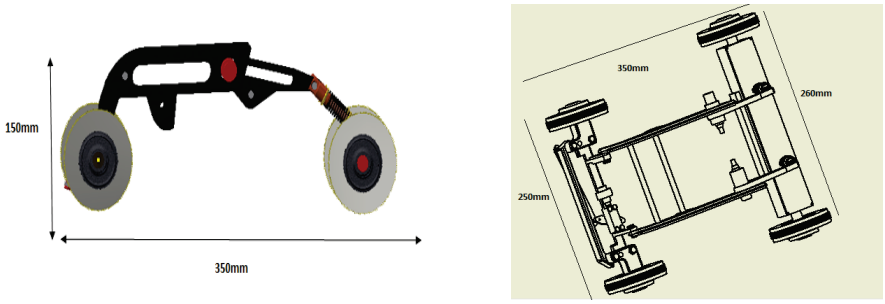

Fig. 4. Designed model of Inspection Robot

The designed robot is fabricated with a lightweight aluminium frame and consists of four magnetic wheels operated by geared DC motor. To keep the flexibility, the servo joint is provided in the aluminium frame so that the robot can expand and contract its structure.

It consists of a front axle with DC geared motors mounted with a gearbox to provide high torque to the front wheels. This robot is teleoperated so that the inspection person can operate it from a remote location. A receiver module on the robot structure and the transmitter module on the remote inspector side helps maintain a wireless communication of 2.4 GHz to control the robot from a remote location.

Table 1

Dimensional specifications of the robot

Parameter	**Value**
Length	35 CM
Width	25CM
Height	15CM
Locomotion	Magnetic wheeled
Control Operations	2.4 GHZ Remote Control unit
Drive	4 motors. 4WD
Approx. Total Weight without battery	4 kg (approx.)
Maximum Travel Speed	NA
Battery	Lithium Polymer 1000mah
Controller	Raspberry pi
Operating voltage	12 V

Table 2

Input and output parameters of robot

Input Parameters	Output Parameters
Total Mass of robot = 4 kg	Minimum Angular velocity = 15 rpm
Number of drive motors = 2 efficiency	Required torque = 1.5 Nm at 90%
Radius of drive wheel = 3 inch	Maximum current = 0.2980 A
Robot velocity = 0.1 m/s	Battery pack = 0.198 Ah
The maximum inclination angle = 90 degree	
Supply voltage = 7 volts	
Desired acceleration = 0.1 m/s2	
Desired operating time = 20 mins.	

DC geared motors are controlled by electronic speed control(ESC) devices and can be controlled wirelessly from remote locations. The unit of shock absorbers is placed at the rear axle to minimize the shocks for the smooth movement of the robot. The rear axle also consists of a DC geared motor with a gearbox to provide rotational torque to the rear wheels. A steering mechanism is embedded into the front axle to turn the structure of the robot. A servomechanism is placed between the chassis of robots to provide access to robots on the concave and sharp corners. A rotational joint in between the chassis offers an extra degree of freedom. The servo motor is programmed so that during the bump or sharp corners, it will rotate so that the rear axle comes closer to the front axle. By doing that robot can maintain some height to pass the sharp corners.

The different phase of robot motion has been presented in the below Fig. 5. Here, it is visible that the robot can easily avoid the corner obstacles by contracting and expanding the flexible structure.

Phase 1: The inspection robot performs the climbing operation on a ferromagnetic steel structure by using the magnetic wheeled locomotion

Phase 2: An operational obstacle avoidance mechanism can be seen during phase 2 of robot movement. The robot is bending the chassis by moving the rear wheels' axle near the front axle wheel. The movement of the rear wheels to the front wheels was achieved by keeping the front wheel stationary and moving the rear axle near the front axle. The chassis bending was performed by a joint provided with a servo motor. So by doing this robot can avoid the corner obstacles.

Phase 3: After crossing the corner obstacle, the robot can expand the chassis so it can easily roll on the surface.

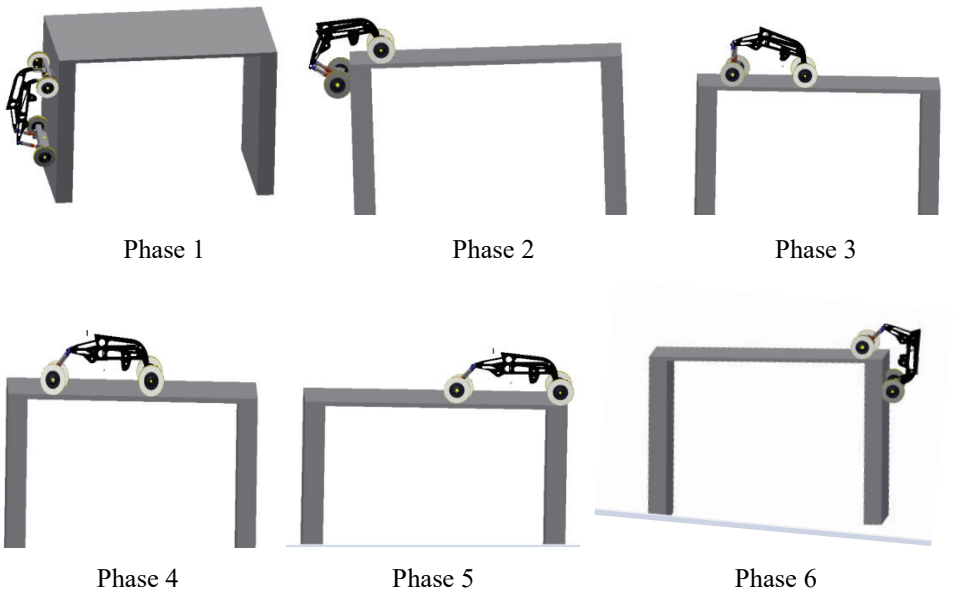

Fig. 5. Various modes of operation on a bridge

Phase 4: Extension of robot chassis is presented in phase 4. Similarly, like phase 2, extension was performed on rear axle of robot.

Phase 5: In phase 5 robot performs the inspection process on a plain surface area using the GMR sensor array.

Phase 6: In phase 6 robot detects the corner edge and starts preparing to avoid the corner obstacle similarly, as explained in phase 2.

During all phases of robot motion, the robot performs the inspection process and streams a live video, with a real-time crack detection graph to a remote location.

4. Components used for Robotic system

In this section, the block diagram of the project and the design aspect of independent modules are considered. The Block diagram is shown in fig. 6.

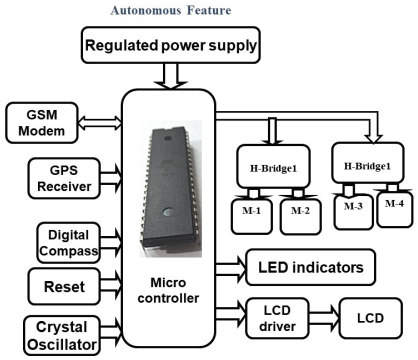

Fig. 6. Autonomous features of crack detection robots

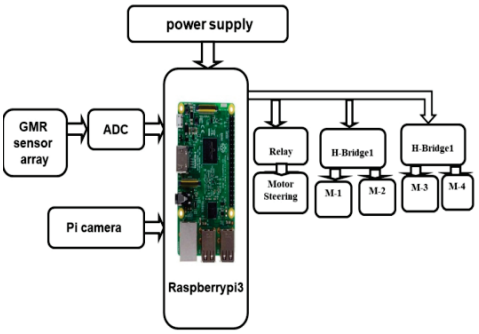

Fig. 7. Systematic diagram of the robot

The main blocks of the Autonomous crack detection robot are:

1. Power Supply.
2. Microcontroller.
3. Raspberrypi3 processor.
4. DC motors with drivers.
5. GSM
6. GPS
7. Crystal oscillator.
8. Reset.
9. LED Indicators
10. Pi camera.
11. Digital compass.
12. LCD
13. GMR Sensors
14. Relay

4.1. Microcontroller

Microprocessors and microcontrollers are widely used in embedded systems products. The microcontroller is a programmable device. It has a CPU in addition to a fixed amount of RAM, ROM, I/O ports and a timer embedded on a single chip. The fixed amount of on-chip ROM, RAM and number of I/O ports in microcontrollers make them ideal for many applications in which cost and space are critical.

The microcontroller used in this project is PIC16F877A. The PIC families of microcontrollers are developed by Microchip Technology Inc. The features of PIC16F877A are 256 bytes of EPROM data memory, self-programming, an ICD, 2 Comparators, 8 channels of 10-bit Analog-to-Digital (A/D) converter, 2 capture/compare/PWM functions, and the synchronous serial port that can be configured as either 3-wire Serial Peripheral Interface (SPI™) or the 2-wire Inter-Integrated Circuit (I²C™) bus and a Universal Asynchronous Receiver Transmitter (USART). All of these features make it ideal for more advanced level A/D applications in automotive, industrial, appliances, and consumer applications.

Fig. 8. Microcontroller

4.2. Rechargeable Battery Power Supply

A rechargeable battery, storage battery, secondary cell, or accumulator is a type of electrical battery that can be charged, discharged into a load, and recharged many times. It is composed of one or more electrochemical cells. The term "accumulator" is used as it accumulates and stores energy through a reversible electrochemical reaction.

Fig. 9. Rechargeable battery

Specification of the Power supply

- Very Small in size and weight compared to Ni-Cd, Ni-MH and Lead Acid Batteries
- Full Charge for 180 minutes with a special charger
- Long life with full capacity for up to 1000 charging cycles
- 3X Li-Po 3.7V 2200mAh cells (3S1P)
- Low maintenance
- 195 Grams Weight
- Volume: 10.5cm*3.3cm*2.2cm
- Discharge Current: 40*2200maH = 88Amp
- Max Charging Current: 1A

4.3. LED of the Robot

LEDs are semiconductor diodes that allow the circuit current to flow in a particular direction. The formation of a PN diode occurs by adding two different materials. At a PN junction, the P side is rich in positive charge and lacks electrons. The N side consists of the excess of electrons and lacks a positive charge. The internal structure and parts of the led are shown below fig. 10.

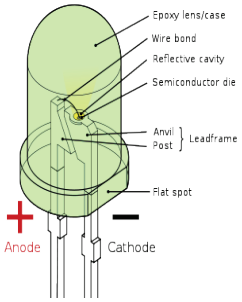

Fig. 10. Parts of the LED

4.4. Global Positioning System (GPS) MODULE

Ublox NEO-6M GPS module with an antenna is a cost-effective and high-performance GPS. This module is very compact (22*30 mm) and offers a wide range of connectivity options as battery consumption is always the main concern for mobile robots. NEO-6M compact architecture, less power consumption and memory options withdraw attention to make it ideal for the operation of battery-based mobile robots. The compact size of NEO-6 M provides a feature of easy mounting in space-constrained areas.

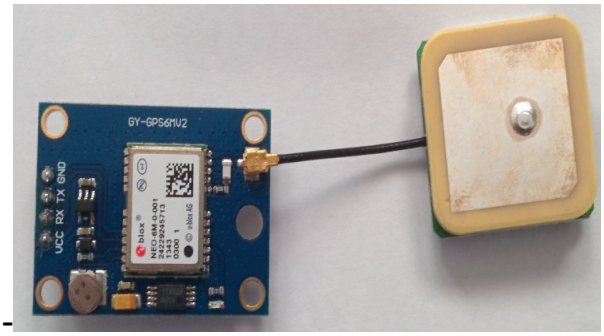

Fig. 11. NEO 6M GSM Module

- Ublox NEO-6M GPS Features and Specifications: Standalone GPS receiver
- U-Blox NEO-6M GPS module
- Build-in 18X18mm active GPS antenna
- UART TL socket
- RTC crystals on board for faster warm and hot starts
- Rechargeable battery for Backup
- Dimension: 22 mm × 30 mm
- Height: 13 mm
- Weight: 12 g/14.4 g (include cable)
- Hole diameter: 3 mm

4.5. GSM Global Systems for Mobile Communication (GSM)

In this manuscript, we have used a GSM modem SIM300 to make the system more autonomous. SIM300 GSM Modem has a serial interface with plug and play facility. Using this modem for autonomous crack detection, robots can be used to send SMS, receive and make calls with the help of an AT command. For interfacing this modem with the microcontroller, an RS232 interface is used. The GSM modem is equipped with a SIM holder, power regulation and an external antenna.

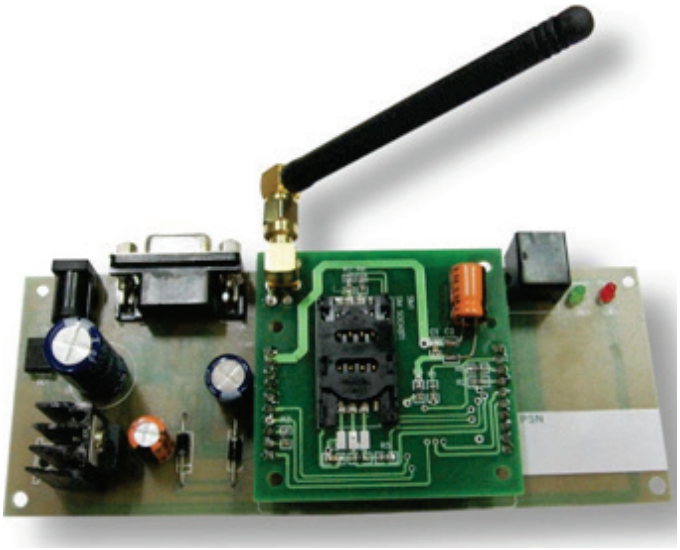

Fig. 12. SIM300 GSM Module

Figure 13 demonstrates the connection diagram of the autonomous crack detection robot. From fig. 13, it can be seen that four DV geared motors are connected to the ARM-11 Raspberry pi processor. Four DC geared motors generate enough torque to rotate the wheels in the inspection area.

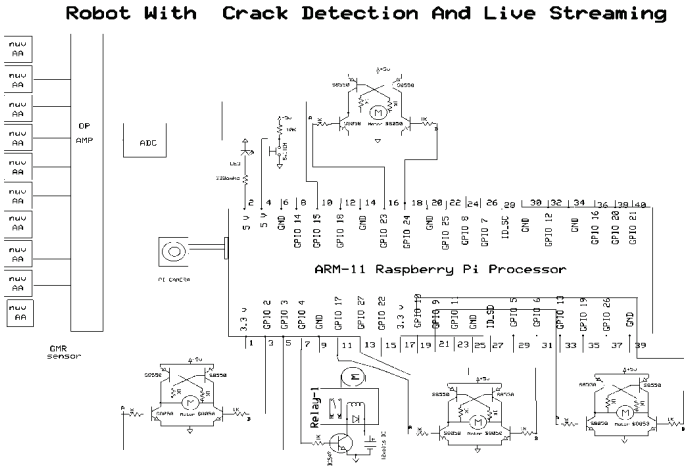

Fig. 13. Architecture of crack detection robot

Figure 14 shows the flow diagram of the whole inspection process and robot motion. In the first phase, it verifies that the robot is connected with the proper communication method. Once the robot is connected to Wi-Fi, it initiates the communication module and starts processing the live video streaming, GMR sensor array graphical results to a remote server location.

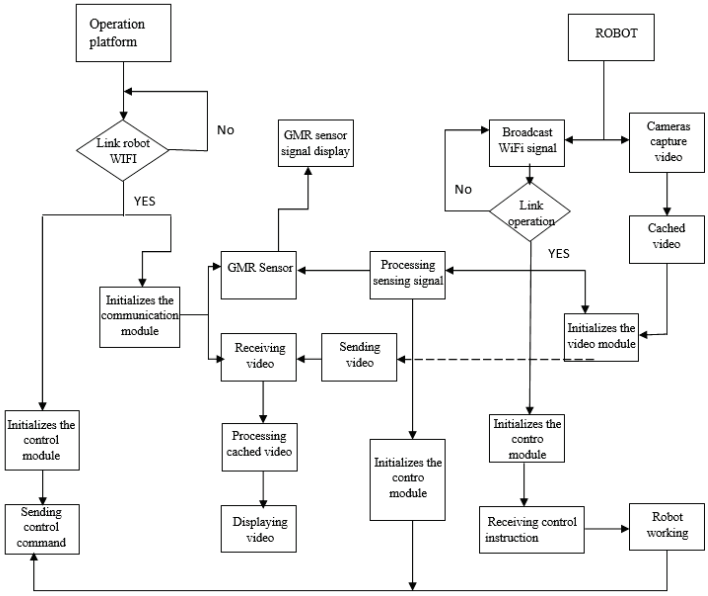

Fig. 14. Flow Diagram of Robotics system

4.6. GMR (Giant Magnetoresistance) Sensor Array

A GMR sensor array was developed to examine the loss of metal caused by the influence of corrosion on the steel surface of overhead crane bridges. The arrangement of the GMR sensor array is presented below in fig. 15.

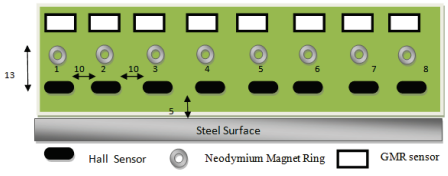

Fig. 15. Channel of GMR Sensor Array

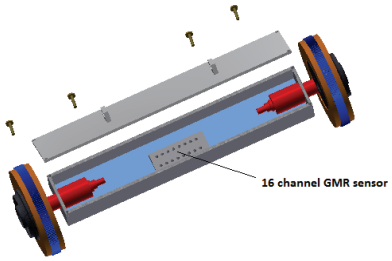

Fig. 16. Positioning of GMR sensor on the front axle

The whole concept of the design of the GMR sensor array consists of 8 hall sensors, circular permanent magnet rings of Neodymium and 8 GMR sensor of NVE AA-005-02. All the components are mounted on PCB (printed circuit board). Magnetic rings are placed just above the hall Sensors. To capture better quality results, the distance between the steel surface and the GMR sensor array is 5 mm. To keep the magnetic field uniform on the steel surface, all the magnetic rings and hall sensors are placed at an equal distance. In fig. 15, the position of the designed GMR sensor array is placed between two magnetic wheels that also contribute to magnetizing the steel surface. As mentioned earlier in the section, the wheel consists of a permanent magnet and generates a uniform magnetic field on the specimen surface during the rotation of the wheel. For better understanding, fig. 16 represents the placement of the GMR sensor on the robot chassis.

In the case of the movement of the robot, the specimen area will get magnetized uniformly.

In the presence of corrosion in the steel area, the magnetic field will be lesser than the area without corrosion. Corroded areas cannot be magnetized well. As a result, the magnetic flux density will be smaller in that area. The detection of corrosion can be identified by calculating the difference in magnetic flux by using the hall sensors. To perform the accuracy check on the designed GMR sensor array, first, a software analysis was performed using FEMM (Finite Element Method Magnetics), as presented in fig. 17. In software analysis, the parameters are set as follows: the thickness of specimen steel surface area 10mm, the thickness of permanent magnet on wheel 26mm, and the distance between the steel surface and magnet is 5mm. In one instance, in the presence of metal loss on the metal

surface, the magnetic lines were distorted, and there was a significant decrease in magnetic field intensity in the area of metal loss.

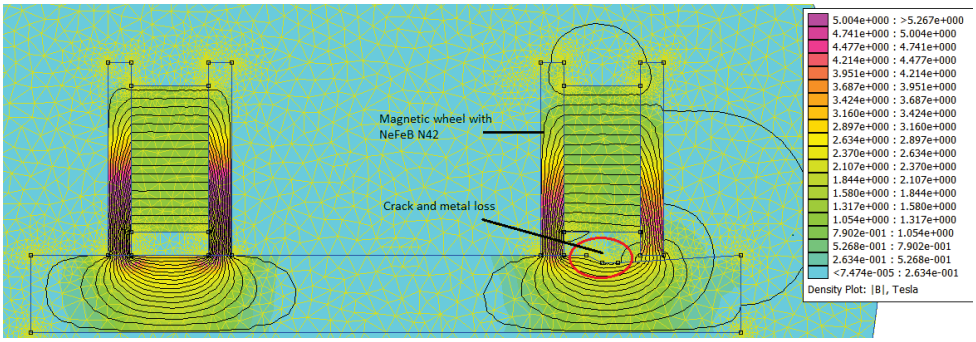

Fig. 17. FEMM method on robotics wheels on inspection area. Left wheel (surface with no defect), right wheel (surface with metal loss)

Additionally, the GMR sensor also identifies the change in magnetic field lines and results can be seen in deviation. Figure 18 represents the graphical results of the GMR sensor array and shows depth and width of crack by using the GMR sensor array.

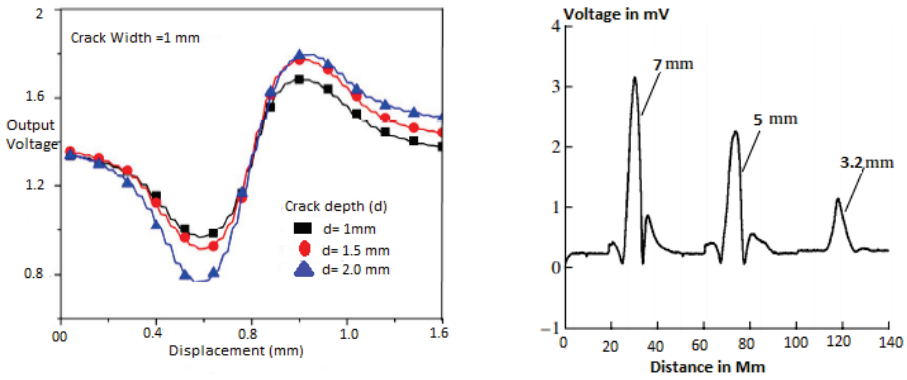

Fig. 18. GMR sensor array results

5. Conclusions and Results

A method of testing the girder of a bridge crane with the use of a specialized measuring type robot. This system employs eight high sensitive GMR sensors mounted on a printed

circuit board in an asymmetrical pattern with hall sensors and permanent magnets. No external excitation source or current is required to induce the magnetic field. The magnetic field was induced by the magnetic wheels of the robot and the small magnets placed above the GMR sensor in the PCB circuit. Instrumentation consists of a power supply circuit (PSC), router to establish wireless communication, Rasberryi3, and GMR sensor array with an analog to digital converter (ADC). In addition, a data acquisition (DAQ) system, ADC Pi, is used to convert the analog sensor signal to a digital signal. The designed system can detect various types of defects by giving a variation in the output of the GMR sensor. If the surface is without defect, the output of the GMR sensor becomes constant. Lesser will be the distance between bridge surface and sensor; larger will be the change in resistance. The output waveforms are in sine forms representing defects with varying shapes, sizes and orientations. The arrangement of GMR sensors are such that it can measure the cracks located at different angles. By using this designed system, it is feasible to identify the fatigue cracks in overhead crane bridges.

Acknowledgement
The work has been financially supported by the Polish Ministry of Education and Science.

6. References

1. Anand Siva G., Rama Krishna S. et.al.: Crack identification and localization in structural beams using numerical and experimental modal analysis – a review. J. Sci. Technol., Vol. 5, 2020, DOI 10.46243/jst.2020.v5.i4.pp62-68.
2. Fernandez R., Gonzalez E., Feliu V.: A wall-climbing robot for tank inspection: An Autonomous prototype. 36th Annual Conference on IEEE Industrial Electronics Safety IEEE, 2010.
3. Fischer W., Tache F., Siegwart R.: Inspection system for very thin and fragile surfaces, based on a pair wall climbing robots with magnetic wheels. Proceedings of the IEEE/RSJ-International Conference on Intelligent Robots and Systems, USA, 2007.
4. Hafid A., Salimi D. et.al.: Analysis and design of crane beam of experimental power plant turbine building. Journal of physics, Conference Series 1198 082031, 2019, DOI 10.1088/1742-6596/1198/8/082031.
5. Hai T.V., Thu N.H., Tuan H.D., Hiu P.V.: Failure probability analysis of overhead crane bridge girders within uncertain design parameters. J. Sci. Technol. Civ. Eng., Vol. 14, DOI 10.31814/stce.nuce2020-14(3)-11.
6. Juraszek J.: Residual magnetic field non-destructive testing of gantry cranes Materials. MDPI, 12 (4) 2019, DOI 10.3390/ma12040564.
7. Kulka J., Faltinová E., Kopas M., Mantič M.: Diagnostics and optimization of crane track durability in metallurgical plant. Diagnostyka, 17, 2016.

8. Kulka J., Mantic M., Fedorko G., Molnar V.: Failure analysis of increased rail wear of 200 tons foundry crane track. Eng. Fail. Anal., 67, 2016, DOI 10.1016/j.engfailanal. 2016.05.032
9. Lanzutti A., Magnan M., Maschio S., Fedrizzi L.: Failure analysis of a safety equipment exposed to EAF environment. Eng. Fail. Anal., 95, 2019.
10. Misiewicz R., Przybyłek G., Więckowski J.: Welding procedure in designing carrying structures of machines, Proceedings of the 14th International Scientific Conference: Computer Aided Engineering, 2019, DOI 10.1007/978-3-030-04975-1_57.
11. Rusiński E., Iluk A., Malcher K., Pietrusiak D.: Failure analysis of an overhead traveling crane lifting system operating in a turbo generator hall. Eng. Fail. Anal., 31 2013, 10.1016/j.engfailanal.2013.02.008.
12. Schoeneich P. et al.: Tubulo – a train-like miniature inspection climbing robot for ferromagnetic tubes. 1st International Conference on Applied Robotics for the Power Industry, 2010, DOI 10.1109/CARPI.2010.5624462.
13. Shen W., Gu J., Shen Y.: Permanent magnetic system design for the wall-climbing robot. Proceedings of the IEEE International Conference on Mechatronics & Automation, Niagara Falls, Canada, July 2005.
14. Sun Y., J Zhai., Zhang Q., Qin X.: Research of large scale mechanical structure crack growth method based on finite element parametric sub model. Eng. Fail. Anal., 102, 2019.
15. Tache F., Fischer W., Caprari G., Siegwart R., Moser R., Mondada F.: Magnebike: A Magnetic Wheeled Robot with High Mobility for Inspecting Complex-Shaped Structures. Journal of Field Robotics, Vol. 26, 2009, DOI 10.1002/rob.20296.
16. Tavakoli M., Viegas C., Marques L., Pires J.N., De Almeida A.T.: OmniClimbers: Omni-directional magnetic wheeled climbing robots for inspection of ferromagnetic structures. Robotics and Autonomous Systems, Vol. 61, No. 9, 2013, DOI 10.1016/ j.robot.2013.05.005.